Heliyon 9 (2023) e17164

Contents lists available at ScienceDirect

Heliyon

journal homepage: www.cell.com/heliyon

How does exercise affect energy metabolism? An *in silico* approach for cardiac muscle

Bahar Hazal Yalçınkaya [a,*,1], Seda Genc [b], Bayram Yılmaz [c], Mustafa Özilgen [d]

[a] *Department of Genetics and Bioengineering, Yeditepe University, Istanbul Turkey*
[b] *Department of Gastronomy and Culinary Arts, Yasar University, Bornova, Izmir, Turkey*
[c] *Department of Physiology, Faculty of Medicine, Yeditepe University, Istanbul, Turkey*
[d] *Department of Food Engineering, Yeditepe University, Istanbul, Turkey*

ARTICLE INFO

Keywords:
Kinetic and thermodynamic analyses
Mitochondrial bioenergetics
Muscle work performance efficiency
Exergy destruction
Entropy generation

ABSTRACT

We explored an *in silico* model of muscle energy metabolism and demonstrated its theoretical plausibility. Results indicate that energy metabolism triggered by activation can capture the muscle condition, rest, or exercise, and can respond accordingly adjusting the rates of their respiration and energy utilization for efficient use of the nutrients. Our study demonstrated during exercise higher respiratory activity causes a substantial increase in exergy release with an increase in exergy destruction, and entropy generation rate. The thermodynamic analysis showed that at the resting state when the exergy destruction rate was 0.66 W/kg and the respiratory metabolism energetic efficiency was 36% and exergetic efficiency was 32%; whereas, when the exergy destroyed was 1.24 W/kg, the energetic efficiency was 58% and exergetic efficiency was 50% during exercise. The efficiency results suggest the ability of the system to regulate itself in response to higher work demand and become more efficient in terms of converting energy coming from nutrients to useable energy when the circulating medium has sufficient energy precursor.

1. Introduction

The prevalence of deaths due to heart disease in the US increased by almost 6% between 2010 and 2016 [1,2]. One of the major causes of heart failure is a decline in muscle efficiency [3–5]. As people age between 20 and 80 years, there is a decline of approximately 25–30% in muscle efficiency [6]. This decline is attributed to the loss of muscle mass and function related to aging [7–9], which in turn rely on mitochondrial functioning to support cellular energetics.

Muscle cell bioenergetics rely mostly on mitochondria, the powerhouses of the cells, that regulates energy supply and energy-sensitive signaling pathways, production, and signaling of reactive oxygen species, calcium homeostasis, and apoptosis [10]. Although under normal cardiac conditions, fatty acid oxidation is responsible for energy flow, where lower glucose metabolism is contributed, under stress conditions, fatty acid oxidation may be reduced and glucose metabolism compensates for energy demand. Energy production occurs in the mitochondria via a relative chemical reaction cascade, tricarboxylic acid cycle (TCA), oxidative phosphorylation, and metabolic transport reactions. Schematic description of the muscle cell is provided in Fig. 1 where, in a cyclic

* Corresponding author.
E-mail addresses: baharhazalyalcinkaya@gmail.com, bahar.selimbeyoglu@nyspi.columbia.edu (B.H. Yalçınkaya).
[1] Present address: New York State Psychiatric Institute and the Department of Psychiatry, Columbia University Irving Medical Center, NY 10032, USA.

https://doi.org/10.1016/j.heliyon.2023.e17164
Received 4 March 2023; Received in revised form 6 June 2023; Accepted 8 June 2023
Available online 13 June 2023

pattern, ATP is produced in the metabolism and then hydrolyzed in the muscle machinery into ADP + P_i to fuel the work performance. The cycle is completed after reconverting ADP + P_i into ATP in the energy metabolism. If sufficient nutrients are provided to the metabolism, the higher the amount of ADP and Pi circulating in the system, the higher will be the ATP production rate, and subsequently, the higher will be the work performance rate. Mammalian cells can change their rate of energy metabolism by adjusting their rates of respiration and ATP utilization, for efficient use of the energy or exergy extracted from the nutrients [11]. The conversion efficiency of the chemical energy into mechanical power in the muscle is not constant and shows variability due to changes of physiological conditions of the muscle, like temperature, ion concentration in the medium and the age of the subject, the amount of nutrients (e.g. glucose, ADP) etc. Under the steady state conditions, the ATP production and hydrolysis rates are balanced. Muscle work efficiency η_{muscle} is described (Eq. (1)) as a combination of the metabolic efficiency of ATP production, $\eta_{metabolism}$, and the mechanical efficiency of the work performance by the muscle fibers, $\eta_{mechanical}$ [12],:

$$\eta_{muscle} = (\eta_{metabolism})(\eta_{mechanical}) \tag{1}$$

In equation (1), η_{muscle} is referred to as the first law muscle work efficiency and defined as (energy utilized by the muscle for work performance)/(energy extracted from the nutrients). In this definition $\eta_{metabolism}$ is defined as the (energy of the ATP produced in the energy metabolism)/(energy of the nutrients allocated for the ATP production) and $\eta_{mechanical}$ is defined as the (work performed by the muscle)/(energy of the ATP produced in the energy metabolism). When the terms of equation (1) are expressed in terms of exergy, instead of energy, η_{muscle} is referred to as the second law muscle work efficiency. Metabolic efficiency, $\eta_{metabolism}$, was used to evaluate ideal muscle work performance [13] and the brain energy metabolism [14–16] and has been the subject of numerous experimental studies [4,17,18].

The laws of thermodynamics have an informative role in the analysis of systems and devices where energy transfer and transformation occur. The conversion of chemical energy into mechanical energy and heat constitute a thermodynamic system. The living systems convert chemical energy into mechanical work and heat for several tasks e.g. movement, respiration, and thermal regulation, etc. Muscle is a thermodynamic device that is able to transduce chemical energy coming from metabolism into mechanical energy. Muscle bioenergetics provide insight to how much chemical energy is used to expand work and how this energy transaction varies in different conditions. Therefore, it is appropriate to describe muscle energetics in thermodynamic terms. Thermodynamic assessment reveals how efficiently a system is performing under the prescribed conditions. Exergy is a theoretical maximum useful energy that can be extracted from a system to perform work. Experimental and theoretical [13] approaches of muscle efficiency estimations may help to assess the degree of muscle loss, the effect of aging and longevity. Estimating exergy efficiencies of a system or subsystem is more informative than estimating energy efficiencies since energy flow from/to a system is regulated by the exergy content of the system. Exergy analysis helps to separate inefficiencies of the system that occur due to effluent losses and those due to irreversibilities. Fundamental principles of thermodynamics including exergy analysis have been extensively used to study metabolism [12,19–23] and systems interaction with surroundings within the context of thermal body comfort [24,25], aging or the effect of the physical activity level on lifespan entropy generation [26–28]. In mammalian cells, energy balance regulation of metabolism has long been a subject of investigation, in particular, regulation of mitochondrial energy synthesis has been a prior interest [16,29]. Mitochondrial metabolism fulfills kinetically and thermodynamically complex tasks under normal condition, excess food, starvation, and control of ATP production. In those conditions the mitochondrial respiratory activity is controlled by the amount of ADP and phosphate available in the

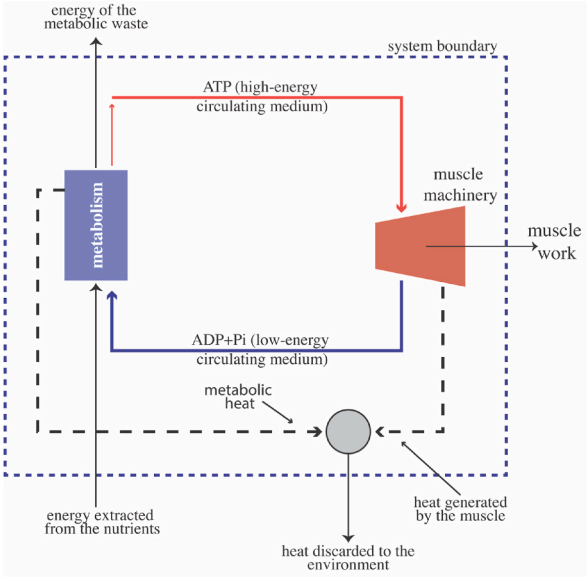

Fig. 1. Schematic representation of the skeletal or cardiac muscle cell energetics.

cell. In the literature although the overall work performance efficiency of the muscle cell, η_{muscle}, in eq (1), has been studied, there are only very limited studies regarding the effect of the availability of the energy precursor ADP on the efficiency of the muscle machinery.

An impulse ATP input to mitochondria was employed to represent the operating conditions of the muscle machine and the response of the system to these impulses were simulated. When the Gibbs free energy change of a system is zero, the ATP production and hydrolysis rates will be balanced, implying that the ATP hydrolysis and synthesis take place at the same rate. In healthy cells, Gibbs free energy is far from equilibrium with their environment, which enables cells to hydrolyze the pre-synthesized metabolic ATP to fulfill intra- and extracellular tasks [16].

This study tries to find an answer to the question of "how efficiently the muscle system uses this energy precursor availability for the demands of energy production?''considering different conditions. In this proof of concept, we make use of cascades of metabolism (e.g., glycolysis and the production of energy carrying molecules) via *in silico* models to explore cardiac muscle system and respiratory activity in terms of thermodynamic indicators, including energy and exergy efficiencies, at rest and during moderately intense treadmill exercise (5mph) with normal level and higher level of energy precursor in the circulating medium, respectively. Kinetic and thermodynamic models of metabolism showed that a higher amount of energy precursor, ADP, availability during exercise accompanied with larger amounts of ATP utilization to fulfill work demand which leads to higher amounts of oxygen consumption and heat release due to higher intensity of the metabolism leaving the system energetically and exergetically more efficient. Higher thermodynamic efficiency analyses point to the muscle systems ability to regulate itself to energy or substrate availability and work conditions.

2. Material and methods

2.1. The muscle system

A model depicting the kinetics of a muscle cell is presented through a set of reactions, which include those involved in the TCA

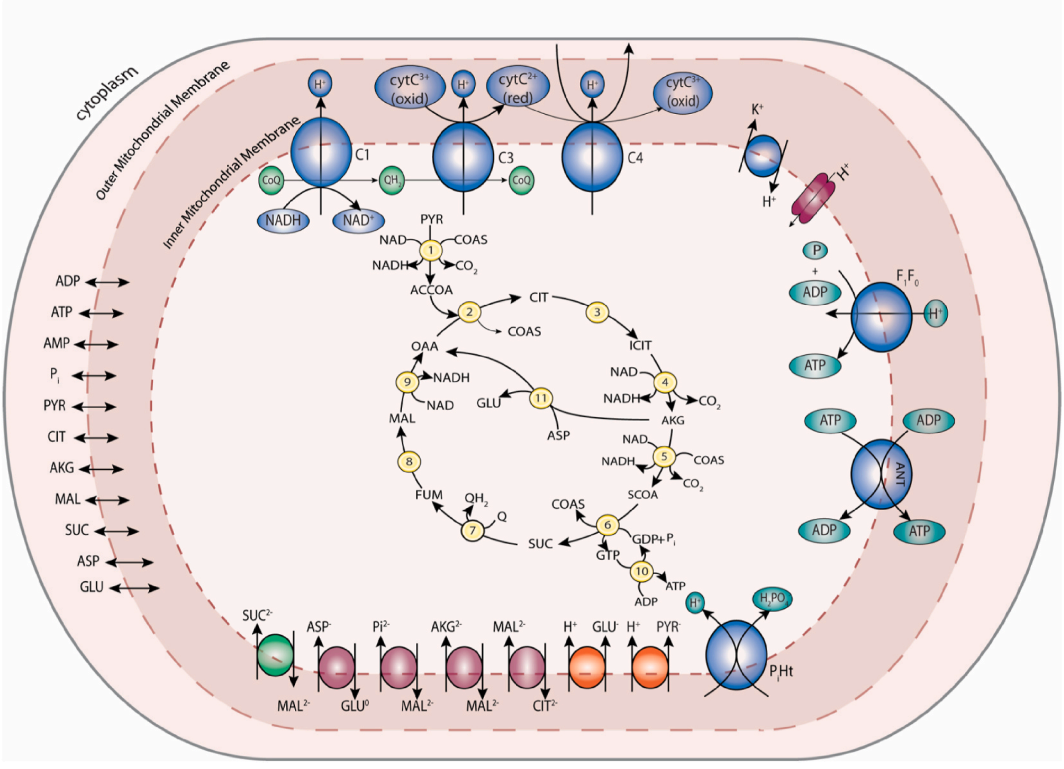

Fig. 2. Schematic representation of the flow diagram of the metabolites: (1) pyruvate dehydrogenase; (2) citrate synthase; (3) aconitase (4) isocitrate dehydrogenase; (5) α-ketoglutarate dehydrogenase; (6) succinyl-CoA synthase; (7) succinate dehydrogenase; (8) fumarase; (9) malate dehydrogenase; (10) nucleoside diphosphokinase; (11) glutamate oxaloacetate transaminase; (C1) complex I; (C3) complex III; (C4) complex IV; (ANT) adenine nucleotide translocase and (F_1F_0) F1-Fo ATPase. ACCOA, acetyl-CoA; ATP, adenosine triphosphate; ADP, adenosine diphosphate; AMP, adenosine monophosphate; ASP, aspartate; AKG, α-ketoglutarate; CIT, citrate; $CytC^{2+}$ (oxid), oxidized cytochrome C; COQ, oxidized ubiquinol; $CytC^{2+}$ (red), reduced cytochrome C; (QH_2), reduced ubiquinol; COAS, CoA-SH; GLU, glutamate; GTP, guanosine-5′-triphosphate; GDP, guanosine-5′-diphosphate; NAD, nicotinamide adenine dinucleotide; NADH, reduced form of nicotinamide adenine dinucleotide; PYR, pyruvate; OAA, oxaloacetate; ICIT, isocitrate; SCOA, succinyl-CoA; SUC, succinate; FUM, fumarate; MAL, malate; CO_2, carbon dioxide; Pi, inorganic phosphate. (For interpretation of the references to colour in this figure legend, the reader is referred to the Web version of this article.)

cycle, pyruvate dehydrogenase reaction, oxidative phosphorylation cascade, passive movement of metabolites from the cytoplasm to the inner-membrane, anti-transporter reactions from the inner-membrane to the matrix, H+ leakage, H2PO4-/H+ cotransporter activity, as well as metabolite exchange reactions (antiports) and transport fluxes shown in Fig. 2. The model also incorporates hexokinase activity, which is essential for the phosphorylation of six-carbon sugars to initiate glycolysis as the first step in breaking down glucose to extract energy for cellular metabolism.

2.2. Kinetic and thermodynamic analyses

Kinetic model of Wu et al. [34], was employed with ex vivo measured enzyme activity and transporter-kinetic parameters adapted from an isolated heart mitochondrion [30,31] and an in vivo skeletal muscle [32,33]. The model simulated unsteady state passive permeation, anti and co-transport, oxidative phosphorylation, and TCA cycle fluxes during both rest (with 0.1 mM ADP concentration) and exercise (with 1.3 mM ADP concentration). Table 1 presents the kinetic reactions for the TCA cycle and oxidative phosphorylation in the model. The metabolic pathway of the respiratory chain was simulated using the COPASI modeling platform with the deterministic Livermore ordinary differential equation solver, with a time step of 0.5 ms for 30 s. The model included variations in the concentrations and fluxes of metabolites involved in the pyruvate dehydrogenase reaction, oxidative phosphorylation cascade, passive permeation of metabolites from the cytoplasm to the inner-membrane, anti-transporter reactions from the inner-membrane to the matrix, H+ leakage, and H2PO4-/H+ cotransporter activity. The model also accounted for hexokinase activity, which is necessary for the initiation of glycolysis, the first step in the breakdown of glucose for cellular metabolism.

The kinetic model combined with the laws of thermodynamics to investigate systems responses. Thermodynamic properties of the metabolites such as transformed Gibbs free energy of formation, standard transformed enthalpy of formation and chemical exergies were determined at the physiological temperature, pH and ionic strength (Table 2). The model was built on several assumptions, including the system functioning under unsteady-state conditions with moving boundaries, aerobic respiration being the dominant glucose metabolism pathway, and all model reactions following Michaelis-Menten enzyme kinetics, passive permeation or rapid equilibrium random Bi–Bi mechanism for aspartate and glutamate transport [34]. The system was isothermal with a uniform temperature (T = 310.15 K) distributed throughout the subsystems, and the environmental temperature set to T0 = 298.15 K. The system boundaries allowed for mass and energy transfer and defined the control volume. Furthermore, the mechanical power of the system was determined based on the cardiac cycle of a 45 kg miniature Yucatan swine [35], and it was assumed that the cardiac cells completely oxidize pyruvate.

The transformed Gibbs free energy of formation, $\Delta g^T_{f,j}$, transformed enthalpy of formation, $\Delta h^T_{f,j}$, and chemical exergy, $b_{ch,j}$, of each metabolite are calculated as described by Alberty 2005 [36] under the conditions prevailing in the muscle ($pH = 7.27, T = 310.15K, and\ I = 0.14M$) and listed in Table 2. Transformed Gibbs free energy of formation and standard transformed enthalpy of formation of the metabolites are calculated at the physiological conditions as:

$$\Delta g^T_{f,j} = \frac{T}{T_0}\Delta g^0_{f,j} + \left(1 - \frac{T_0}{T}\right)\Delta h^0_{f,j} - \frac{RT\alpha(T)I^{\frac{1}{2}}}{1 + B_e I^{\frac{1}{2}}}\left(z_j^2 - n_{H,j}\right) - n_{H,j}\Delta g^0_{f,H^+} + 2.303 n_{H,j} RTpH \tag{2}$$

$$\Delta h^T_{f,j} = \Delta h^0_{f,j} + \frac{RT\beta I^{\frac{1}{2}}}{1 + B_e I^{\frac{1}{2}}}\left(z^2 - n_{H,j}\right) \tag{3}$$

where α is Debye-Hückel constant ($kg^{1/2}mol^{-1/2}$), β is the coefficient for ionic strength, n is the number of hydrogen atoms, R is ideal gas constant (J/Kmol), T is temperature (^{0}K), B_e is empirical constant in the extended Debye-Hückel equation ($kg^{1/2}mol^{-1/2}$) and z is

Table 1
TCA cycle and oxidative phosphorylation metabolic reactions occurring in a muscle cell. Cytoplasm, inner-membrane and mitochondria donated as subscripted c, i and x, respectively.

Enzyme	Reactions	Δh_{rxn} (kJ/mol)	Δg_{rxn} (kJ/mol)
Hexokinase	$GLC_c + ATP_c \rightarrow G6P_c + ADP_c + H_c$	−22.42	−20.71
Pyruvate dehydrogenase	$PYR_x + COAS_x + NAD_x \rightarrow ACCOA_x + NADH_x + CO_{2x} + H_x$	−127.42	−182.12
Citrate synthase	$ACCOA_x + OAA_x + H_20_x \rightarrow CIT_x + COAS_x + 2H_x$	−1321.99	−47.89
Aconitase	$CIT_x \rightarrow ICIT_x$	1515.17	6.65
Isocitrate dehydrogenase	$ICIT_x + NAD_x + H_20_x \rightarrow AKG_x + CO_{2x} + NADH_x + 2H_x$	−532.98	−7.54
α-ketoglutarate dehydrogenase	$AKG_x + CoA_x + NAD_x \rightarrow SCoA_x + CO_{2x} + NADH_x + H_x$	−724.33	−188.90
Succinyl-CoA synthetase	$SCoA_x + GDP_x + Pi_x \rightarrow SUC_x + CoA_x + GTP_x$	−599.23	0.85
Succinate dehydrogenase	$SUC_x + COQ_x \rightarrow FUM_x + QH_{2x}$	131.30	−1.35
Fumarase	$FUM_x + H_2O_x \rightarrow MAL_x$	−1277.11	−3.59
Malate dehydrogenase	$MAL_x + NAD_x \rightarrow OAA_x + NADH_x + H_x$	2215.30	25.96
Glutamate oxaloacetate transaminase	$ASP_x + AKG_x \rightarrow OAA_x + GLU_x$	−27.65	−1762.69
Complex I	$NADH_x + COQ_x + 5H_x \rightarrow NAD_x + QH_{2x} + H_i$	30.55	−66.51
Complex III	$QH_{2x} + 2Cox_i + 2H_x \rightarrow COQ_x + 2Cred_i + 4H_i$	−2.77	−39.64
Complex IV	$2Cred_i + 0.5\ O_{2x} + 4H_x \rightarrow 2Cox_x + 2H_i + H_2O$	−182.55	−116.40
F1F0-ATPase	$ADP_x + Pi_x + H_x + 3H_i \rightarrow ATP_x + H_2O_x + 3H_x$	−116.76	−38.93
Overall TCA	$PYR + 4NAD + COQ + ADP + Pi + 5H2O \rightarrow 4NADH + QH_2 + ATP + 3CO_2 + 4H$	−212.61	−356.59

Table 2
Concentration and thermodynamic properties of the metabolites under biophysical conditions ($pH = 7.27, T = 310.15K, and\ I = 0.14M$) in the muscle cell at condition during exercise by experimentally adding extra free ADP while ATP synthesis is taking place.

Metabolites	$\Delta h^T_{f,j}$ (kJ/mol)	$\Delta g^T_{f,j}$ (kJ/mol)	B_{ch} (kJ/mol)	$RTln(c)$ (kJ/mol)		$B_{ch} + RTln(c) + \Delta g^T_{f,j}$ (kJ/mol)	
				$T = 0s$	$T = 30s$	$T = 0s$	$T = 30s$
ACCOA	−1.04	−48.68	12672.5	−65.08	−53.45	12558.74	12570.37
ADP	−2627.26	−1386.14	5851.38	−29.70	−30.73	4435.54	4434.51
AKG	0.00	−620.74	2061.23	−62.55	−47.43	1377.94	1393.06
ASP	−945.14	−433.25	1783.55	−41.02	−47.90	1309.28	1302.40
ATP	−3617.35	−2253.27	6720.93	−38.38	−32.58	4429.28	4435.08
CIT	−1513.82	−949.79	2475.46	−53.76	−52.57	1471.91	1473.10
CO_2	−692.25	−543.72	414.23	−27.74	−27.74	−157.23	−157.23
COASH	−0.20	−4.59	11850.04	−33.72	−33.18	11811.73	11812.27
COQ	−31.12	3950.32	22734.82	−29.03	−31.64	26656.11	26653.50
Cox	3.11	−6.52	16352.69	−33.39	−34.11	16312.79	16312.06
Cred	1.38	−27.41	16352.69	−47.50	−36.97	16277.78	16288.31
FUM	−776.70	−516.99	1648.98	−51.36	−36.64	1080.63	1095.35
G6P	−2278.85	−1277.03	3343.03	−71.29	−70.95	1994.71	1995.05
GDP	−2627.26	−1386.14	5851.38	−31.49	−32.51	4433.75	4432.73
GLC	−1266.34	−389.19	2473.47	−53.47	−53.47	2030.81	2030.81
GLU	−982.31	−347.06	2653.41	−31.20	−32.03	2275.15	2274.32
GTP	−3617.35	−2253.27	6720.93	−57.53	−34.67	4410.13	4433.00
H_2O (aq)	−191.86	−149.41	1.99	−41.58	−41.58	−189.00	−189.00
ICIT	1.35	−943.14	2475.46	−59.70	−61.97	1472.62	1470.35
MAL	−2245.67	−669.99	1650.97	−56.06	−32.02	924.92	948.96
NAD	−8.65	1140.48	10372.87	−36.52	−39.65	11476.83	11473.70
NADH	−39.89	1204.85	10372.87	−53.47	−37.43	11524.25	11540.29
O_2	−11.7	17.53	3.97	−42.70	−42.70	−21.20	−21.20
OAA	0.87	−708.40	1650.97	−66.51	−62.53	876.06	880.04
Pi	−1298.71	−1055.47	871.54	−52.25	−35.91	−236.18	−219.84
PYR	−596.91	−341.32	1236.74	−53.47	−62.44	841.95	832.98
QH_2	−31.81	3948.18	22734.82	−60.06	−36.04	26622.93	26646.95
SCOA	−1.04	−334.88	13497	−35.90	−37.92	13126.22	13124.20
SUC	−908.69	−517.78	1648.98	−57.82	−34.85	1073.38	1096.35

valence. At a given pH some biochemical species like ATP can be at different valence states like ATP^{4-}, ATP^{3-}, and ATP^{2-}. The standard Gibbs free energy of these species were calculated as the sum of the Gibbs free energies of each fraction. The pH of the mitochondrial matrix of the cell is calculated via; $pH = -log[H^+]$ and assumed to be constant through the simulation time and ionic strength is estimated considering the ionic gradient of a mitochondrial matrix of the cell [37].

Exergy of a metabolite is the sum of the exergies of its elements, $b_{ch,j}$, transformed Gibbs energy of formation, $\Delta g^T_{f,j}$, and its concentration exergy $RTln(c_j)$:

$$b_j = b_{ch,j} + \Delta g^T_{f,j} + RTln(c_j) \tag{4}$$

where, R is the universal gas constant and c_j is the concentration of the j^{th} biomolecule in the solution. In the model, standard transformed enthalpy and standard transformed Gibbs free energy of formation were computed with Wolfram Mathematica 10 by considering the conditions that the system lives in.

Muscle work is performed in periodic contractions with a constant period and intensity. As a result, to perform the thermodynamic analysis of muscle, the governing equations are simplified by cyclic operation

$$\oint \frac{dm}{dt} = \oint \sum (\acute{m})_{in} - \oint \sum (\acute{m})_{out} \tag{5}$$

$$\oint \frac{dE}{dt} = \oint \sum (\acute{mh})_{in} - \oint \sum (\acute{mh})_{out} + \oint \acute{Q} - \oint \acute{W} \tag{6}$$

$$\oint \frac{dB}{dt} = \oint \sum (\acute{mb})_{in} - \oint \sum (\acute{mb})_{out} + \oint \acute{Q}\left(1 - \frac{T_0}{T}\right) - \oint \acute{W} + \oint P_0 \frac{dV}{dt} - \oint \acute{X}_{dest} \tag{7}$$

In eq. (7) the left-hand side $\oint \frac{dB}{dt}$ shows the change of the exergy with time in the control volume. The term $\oint \sum (\acute{mb})_{in} - \oint \sum (\acute{mb})_{out}$ represents the inflow minus the outflow exergies of metabolism, where, b is the stream availability and $\dot{m}$ is the mass flow rate. $\oint P_0 \frac{dV}{dt}$ denotes the surrounding work and is zero since cyclic volume changes occur periodically, $\oint \acute{W}$ is the power performed by the muscle and $\oint \acute{X}_{dest}$ represents the exergy destruction rate in the control volume. In the model, the term $\oint \acute{Q} \sum \left(1 - \frac{T_0}{T}\right)$ refers to the exergy transfer due to heat release via metabolism. Power consumed by the muscle is provided via dissociation of ATP, and calculated in terms

of the oxygen consumption rate as:

$$Power = \Delta h^{T}_{TCA} \times \Omega_{O_2} \tag{8}$$

where, Δg^{T}_{TCA} is the Gibbs free energy of the overall TCA cycle and Ω_{O_2} is the oxygen consumption flux. The efficiency of the muscle is defined as the first law efficiency of the muscle work which is defined in analogy with that of Carnot engine as the ratio of the power performed to the power consumed by the system as:

$$\eta_I = \frac{W}{\Delta H} \tag{9}$$

The second law efficiency is defined as the ratio of the actually produced work to the maximum attainable work as:

$$\eta_{II} = \frac{W}{W_{max}} = \frac{W}{(m_i b)_{in} - (m_i b_i)_{out}} = \frac{W}{\Delta G} \tag{10}$$

3. Results

3.1. Model and motivation

To investigate the relationship between energy precursor availability, work performance, and metabolic pathway behavior in cardiac muscle, we employed a computational model based on a previous study [34]. By defining different levels of energy precursor availability for different work conditions, we simulated the metabolic response of the system during rest with normal level ADP and during exercise with increased ADP availability. Our focus was on aerobic respiration starting with glycolysis followed by the formation of ATP and NADH, which are essential energy transport molecules. The model used the steps of the metabolic pathway schematic described in Wu et al. [34] and the simulation assumptions listed in the Material and Method. The reactions are listed in Table 1. Our objective was to examine how efficiently the muscle system uses energy precursor availability for energy production demands under different conditions. We highlighted the fundamental points of the pathway by investigating these cascades of metabolism under rest and exercise conditions. The results provide insight into the behavior of the metabolic pathway and its relationship with energy precursor availability and work performance.

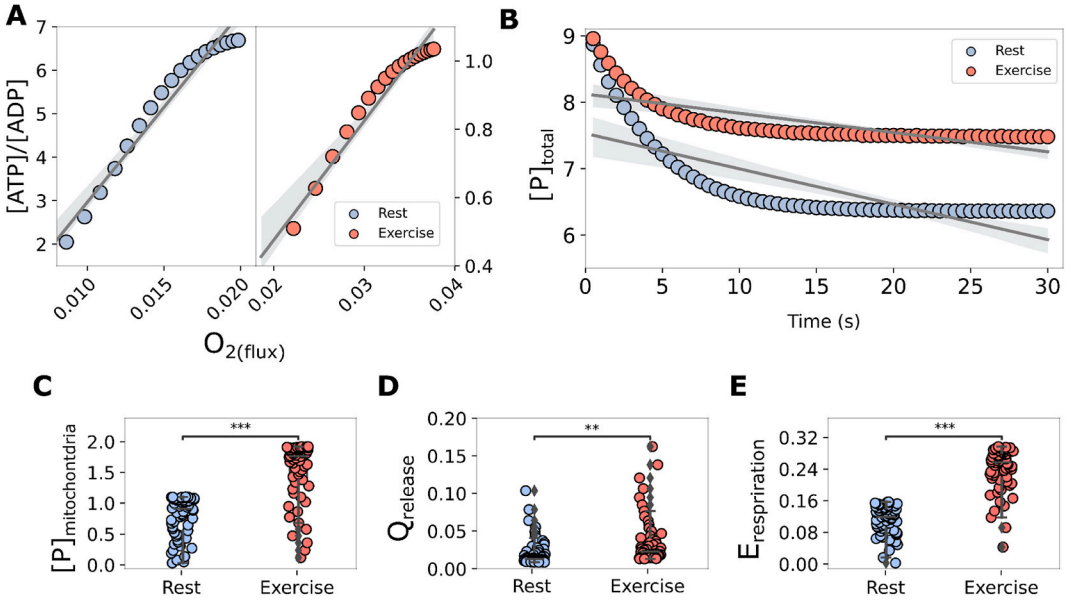

Fig. 3. Using perturbation simulations, we conducted an analysis to investigate changes in phosphate concentration within the mitochondrial matrix and intracellular environment. During our investigation, we discovered (A) that elevated levels of ADP and intracellular inorganic phosphate in the cellular pool have a positive impact on ATP production and oxygen consumption during exercise ($F = 178.29, p \leq 0.001$). These findings indicate that increased ADP and phosphate concentrations contribute to enhanced energy production and higher oxygen utilization during physical activity. (B) Decrease in total concentration of intracellular phosphate and $[P]_{total}$, (mM) was higher during exercise compared to resting conditions ($F = 116.88$, $p \leq 0.001$). Additionally, (C) increase in phosphate concentration within the mitochondrial matrix $[P]_{mitochondria}$, ($F = 101.66$, $p \leq 0.001$) recorded. We quantified the respiration energy by analyzing the rates of oxygen flux through the complex IV reaction and assessing the corresponding Gibbs free energy. (D) An elevation in metabolic heat release $Q_{release}$, within muscle cells during exercise ($F = 9.74, p \leq 0.01$) and (E) higher allocation of energy $E_{respiration}$, during exercise ($F = 225.69$, $p \leq 0.001$). All analyzed by one-way ANOVA (rest versus exercise at corresponding time), *p < 0.05, **p < 0.01, ***p < 0.001, and ****p < 0.0001.

Each metabolite transformed Gibbs free energy of formation, $\Delta g_{f,j}^{T}$, transformed enthalpy of formation, $\Delta h_{f,j}^{T}$, and chemical exergy, $b_{ch,j}$ were calculated under the conditions prevailing in the muscle via Wolfram Mathematica 10 ($pH = 7.27, T = 310.15K, and\ I = 0.14M$) (Eqs. (2) and (3), Table 2). Exergy of a metabolite (Eq. (4)) was calculated by the sum of the exergies of its elements, $b_{ch,j}$, transformed Gibbs energy of formation, $\Delta g_{f,j}^{T}$, and its concentration exergy $RTln(c_j)$.

3.2. Metabolic system thermodynamic analyses

In this study, we investigated the mitochondrial matrix ATP concentration changes response to impulse perturbation (Eq. (11)) via;

$$[\Delta c_{ATP}] = [c_{ATP}]_{final} - [c_{ATP}]_{initial} \tag{11}$$

where 0.04 and 0.39 mM of ATP concentration increase recorded at rest and during exercise, respectively. Fig. 3A shows [ATP]/[ADP] ratio versus the O_2 consumption plots (Ω_{O_2}), peak ratio recorded at 1.2 for [ATP]/[ADP] with 0.037 mmol/s O_2 consumption flux during exercise. Whereas, at rest the peak [ATP]/[ADP] ratio was recorded as 7.0 with the O_2 utilization flux of 0.019 mmol/s, implying that ADP was utilized more efficiently in response to perturbation. Next, we calculated the maximum attainable work performance using the Gibbs free energy change of complex IV reaction. The maximum work performance was found to be 3.5 J/s at rest and 6.8 J/s during exercise. We further calculated the maximum possible metabolic heat removal via enthalpy change of complex IV reaction. At rest metabolic heat removal from the overall reaction was 2.2 J/s and 4.3 J/s during exercise.

Additionally, we calculated the respiration energy from rates of oxygen flux via complex IV reaction and its corresponding Gibbs free energy. We found that more energy was allocated during exercise (Fig. 3E, represented via $E_{respiration}$, one-way ANOVA, $F = 225.69, p \leq 0.001$). Concurrently, we observed an increase in metabolic heat release during exercise of a muscle cell (Fig. 3D, one-way ANOVA, $F = 9.74, p \leq 0.01$).

We conducted an analysis of perturbation simulations to examine changes in phosphate concentration in the mitochondrial matrix and intracellularly. We found that phosphate concentration increased over time in the mitochondrial matrix (Fig. 3C), while the total concentration of intracellular phosphate decreased (Fig. 3B), indicating a decrease in cytoplasmic phosphate concentration. Previous research has shown that intracellular phosphate levels are directly related to ATP hydrolysis and proportional to muscle power output [38]. Our results demonstrate that the total intracellular phosphate ion concentration ($[P]_{total}, mM$) was higher during exercise compared to resting conditions (one-way ANOVA, $F = 116.88, p \leq 0.001$), which led to a higher concentration of phosphate ions in the mitochondrial matrix ($[P]_{mitochondria}, mM$) in muscle cells during exercise. We also compared the adenine nucleotide metabolism [ATP]/[ADP] concentration ratio at rest and during exercise to investigate how nutritional state affects this process. Our findings suggest that higher levels of ADP and intracellular inorganic phosphate in the cell pool enhance ATP production (Fig. 3A) and oxygen consumption (Fig. 3A, one-way ANOVA, $F = 178.29$, during exercise.

First and second thermodynamic laws described (Eq. (5) and (6)) used to analyze the system. Power output (Eq. (8)) was calculated based on systemic and coronary hemodynamic responses of Yucatan swine hearts. The calculations showed that 2.11×10^{-2} W/kg and 6.77×10^{-2} W/kg are produced at rest and during moderately intense exercise (5mph), respectively (Table 3). Exergy destruction rates $X_{destroyed}$ variation with the exergy loss rate X_{loss}, is represented in Fig. 4B via solid line is the linear regression model fit and translucent band lines describe bootstrap confidence intervals generated from the estimate. The exergy loss, X_{loss}, is calculated as demonstrated in Eq. (7), $X_{loss}^{'} = \sum (mb')_{in} - \sum (mb')_{out}$, subtracting the exergy that leaves the system, from exergy that enters the system [40]. There was no significant difference in exergy loss between the two states (Fig. 4E, X_{loss}, p = ns). However, there was an increase in the amount of exergy entering, Ex_{in}, and leaving Ex_{out}, the system during exercise (Fig. 4C and D, one-way ANOVA, $F_{Ex_{in}} = 14.37, p_{Ex_{in}} \leq 0.001$ and $F_{Ex_{out}} = 38.94, p_{Ex_{out}} \leq 0.001$). Endogenous exergy destruction within the system, $X_{destroyed}$ is calculated via Eq. (7). The results showed exergy destroyed during exercise increased due to higher metabolism and power output compared to the resting state (Fig. 4A, represented via, $X_{destroyed}$, one-way ANOVA, $F = 16.34, p \leq 0.001$).

Main findings of this work summarized in Table 5. The energy efficiency of respiration is calculated via:

$$\eta_{energetic\_respiration} = \frac{energy\ released\ via\ ATP\ hydrolysis}{energy\ released\ during\ respiration} \tag{12}$$

Energetic aerobic respiration efficiency of the mitochondrial metabolism is;

$$0.36 = \frac{0.23\frac{W}{kg}}{0.62\frac{W}{kg}} \leq \eta_{energetic\_respiration} \leq \frac{0.68\frac{W}{kg}}{1.18\frac{W}{kg}} = 0.58 \tag{13}$$

Table 3
Cardiac cycle duration and muscle contraction power values at rest and during exercise. Data presented in the table calculated data provided by Bender et al., [35].

	Rest	Exercise
Cardiac cycle duration (s)	0.61	0.23
Power output (W/kg)[a]	2.11×10^{-2}	6.77×10^{-2}

[a] Average weight of a miniature Yucatan swine is 45 kg.

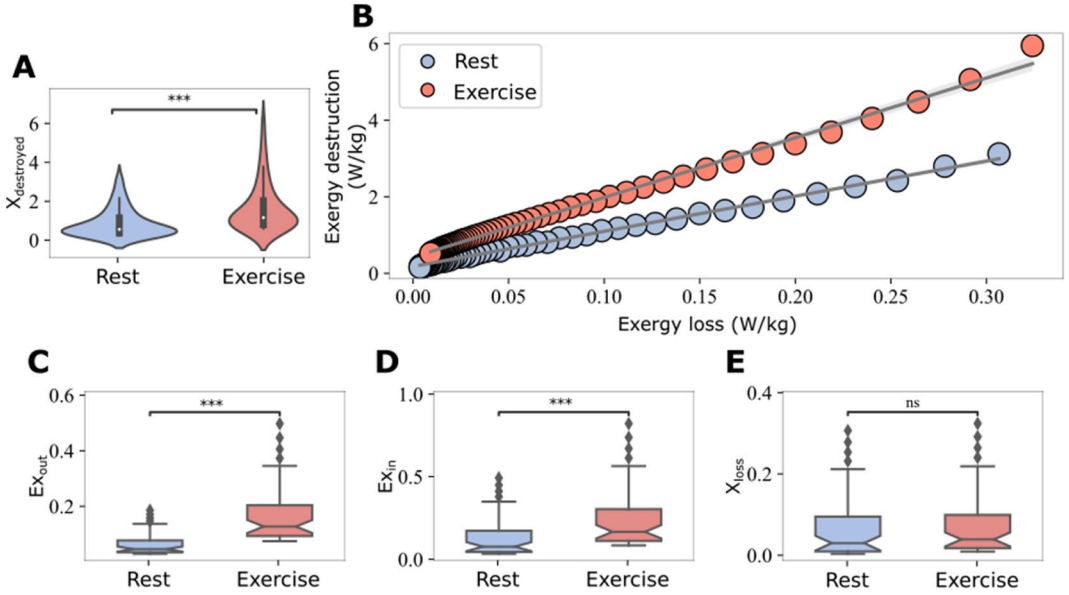

Fig. 4. Thermodynamic analysis showed that (A) exergy destroyed, $X_{destroyed}$, during exercise increased compared to the resting state, primarily due to higher metabolism and power output ($F = 16.34$, $p \leq 0.001$). The first and second laws of thermodynamics (Eq. (5) and (6)) were used to analyze system. (B) To explore the relationship between exergy destruction rates ($X_{destroyed}$) and the rate of exergy loss (X_{loss}), we represented the data using a linear regression model fit (solid line) and generated bootstrap confidence intervals from the estimate (translucent band lines). (C) An increase in the amount of exergy entering the system, exergy inflow, Ex_{in}, a ($F_{Ex_{in}} = 14.37$, $p_{Ex_{in}} \leq 0.001$) and (D) exergy d leaving the system, exergy outflow, Ex_{out}, ($F_{Ex_{out}} = 38.94$, $p_{Ex_{out}} \leq 0.001$) recorded. (E) Exergy loss rate, X_{loss}, shows no difference between conditions ($p = ns$). All analyzed by one-way ANOVA (rest versus exercise at corresponding time), *p < 0.05, **p < 0.01, ***p < 0.001, and ****p < 0.0001.

Table 4
First and Second law of efficiency under the normal and higher amount of ADP at rest and exercise states.

	Rest	Exercise
ADP availability	Normal	Higher
η_I	0.32	0.38
η_{II}	0.13	0.23

Table 5
Summary of the major results of the analysis pertinent to the muscles.

	Rest	Exercise
The total rate of the exergy release in the muscle due to respiratory activity	0.69 W/kg	1.32 W/kg
The rate of the exergy releases due to ATP hydrolysis	0.23 W/kg	0.67 W/kg
Respiratory metabolism energetic efficiency	36%	58%
Respiratory metabolism exergetic efficiency	32%	50%
The ratio of the heat to net energy	0.29	0.24
The ratio of destroyed mitochondrial exergy to cell exergy	0.36	0.49
Exergy destruction in the muscle for 1 mmol ATP synthesis/hydrolysis	0.45 W/kg	0.39 W/kg
Total exergy destruction rate in the muscle	0.66 W/kg	1.24 W/kg
Total entropy generation rate in the muscle	2.1×10^{-3} W/kgK	4.0×10^{-3} W/kgK

Energetic efficiency analysis (Eqs. (12) and (13)) revealed that in rest 36% of the energy potential of aerobic respiration can be converted to work while this efficiency increased to 58% in response to activity. The exergy efficiency of respiration $\eta_{exergetic\_respiration}$ was defined in a similar way as:

$$\eta_{exergetic\_respiration} = \frac{exergy\ released\ via\ ATP\ synthesis}{exergy\ released\ during\ respiration} \tag{14}$$

Exergetic aerobic respiration efficiency of the mitochondrial metabolism is:

$$0.32 = \frac{0.23\frac{W}{kg}}{0.69\frac{W}{kg}} \leq \eta_{exergetic\_respiration} \leq \frac{0.67\frac{W}{kg}}{1.32\frac{W}{kg}} = 0.50 \tag{15}$$

Respiratory metabolism is energetically 22% more efficient during exercise while 18% more efficient exergetically (Eqs. (14) and (15)).

Total exergy destroyed during the process of metabolism (Eq. (16)) within the system boundaries is calculated considering total exergy change of the system and total exergy input and output of the system that are calculated from metabolite fluxes and their exergies.

$$(Total\ exergy\ destroyed) = (Total\ exergy\ inflow) - (Total\ exergy\ outflow) - (Total\ exergy\ change\ of\ the\ system) \tag{16}$$

The end of the simulation time calculations showed that at rest cells consumes 0.69 W/kg of exergy while producing 2.11×10^{-2} W/kg power while 8.71×10^{-3} W/kg exergy is associated with metabolic heat transferred which gives an estimate of the total exergy destruction rate, 0.66 W/kg where 36% its exergy destroyed via mitochondrial metabolism, which corresponds 0.24 W/kg (Table 5). On the other hand, calculations showed during exercise, muscle consumes exergy of 1.32 W/kg while producing 6.77×10^{-2} W/kg cardiac output and transfer 1.32×10^{-2} W/kg exergy via metabolic heat transfer, where the total exergy destruction rate is 1.24 W/kg and 49% of its calculated as coming from mitochondrial metabolism, 0.61 W/kg.

4. Discussion

The analysis of metabolite pathways and thermodynamic systems is mutually beneficial. By frequently measuring the thermodynamics of biological systems at both the molecular and systemic levels, we can gain insights into the efficiency of biological organisms under different conditions [12, 14-16, 20-23, 26-28].

Our *in silico* models, which incorporate detailed metabolic pathways and analyze the thermodynamics of different conditions and systems, reveal how varying levels of energy precursors affect the efficiency of glucose utilization. Specifically, these models can provide valuable information on the factors that facilitate the extraction of more energy and building block molecules from glucose.

Additionally, the analysis of thermodynamic efficiency provides insights into the system's ability to adapt to varying levels of energy or substrate availability and work conditions. To illustrate this, we conducted *in silico* experiments to model the metabolic pathways of the respiratory chain in muscle systems. Specifically, we simulated the system under two conditions: at rest with normal energy precursors, and during moderately intense exercise with higher levels of energy precursor availability. These achieved via considering muscle systems where metabolic pathways of the respiratory chain are simulated by using the COPASI modeling platform with the deterministic Livermore ordinary differential equation solver for 30 s with 0.5 ms time steps. In kinetic models, 42 flux expressions used including unsteady state passive permeation, anti and co-transport, oxidative phosphorylation and TCA cycle fluxes were simulated during rest with 0.1 mM and exercise with 1.3 mM of initial perturbation ADP concentrations [34](Tables 1–2).

Both *in silico* models metabolic pathways are investigated via thermodynamic laws. We showed the impact of system conditions, rest and moderately intense exercise, on maximum attainable work performance rate via Gibbs free energy change of complex IV reaction which showed approximately 2 fold increase during exercise (3.5 and 6.8 J/s at rest and during exercise, respectively). Reconfirming efficient use of ADP at rest. Additionally, maximum possible metabolic heat removal is calculated via enthalpy change of complex IV reaction, showing more metabolic heat needs to be removed from the surface of the body during exercise. These results confirm that metabolic heat released positively proportional to the availability of more ADP in perturbation, and work done by system.

The level of cellular phosphate metabolites is directly linked to the amount of ATP hydrolyzed and is linearly proportional to the muscle system's power output [38]. We examined how the total intracellular and mitochondrial phosphate concentrations change over time in both rest and exercise states. We observed a decrease in the total intracellular phosphate concentration (Fig. 3B) and an increase in the phosphate concentration in the mitochondrial matrix, indicating a decrease in the cytoplasmic phosphate concentration. Our analysis of the total phosphate concentration variation suggests high hexokinase activity in the cytoplasm and high H2PO-4/H+ cotransporter activity from the cytoplasm to the matrix, irrespective of the states.

Free phosphate in the cytoplasm is transported from the cytoplasm to inter-membrane via passive permeation and later used for F1-Fo ATPase activity in the mitochondrial matrix. Total intracellular phosphate concentration significantly higher during exercise, then that of the resting, indicating higher ATP allocation for the power performance during exercise. Model findings point to the presence of a feedback mechanism for the regulation of the ATP synthesis: availability of higher amounts of ATP precursors ADP and intracellular inorganic phosphate in the cell pool enhances the ATP production.

Thermodynamic analysis based on the metabolic reactions indicate that, if a system is ideal, e.g., works with no exergy destruction, $Ex_{destruction} = 0$, the maximum work of 642 kJ may be extracted through utilization of 1 mol of pyruvate, accompanied with 277 kJ of heat removal. During exercise, more oxygen is required to provide greater power since high-intensity metabolism prevails. Respiration energy calculated from rates of oxygen flux via complex IV reaction and its corresponding Gibbs free energy. We have demonstrated that muscle subjected to exercise allocates more energy for respiration (Fig. 3D). Thus, this significant increase in energy allocation during exercise demonstrates an increase in the use of oxygen (Fig. 3A). In order to maintain metabolic demand, more heat is released during exercise (Fig. 3E), when compared to that of at rest.

During our investigation, we opted to use a cardiac system as our model, as most of the kinetic modeling data available is derived from isolated heart mitochondria [30,31], while others were obtained from in vivo skeletal muscle studies [32–34]. All metabolite transformed Gibbs free energy of formation, $\Delta g^{T}_{f,j}$, transformed enthalpy of formation, $\Delta h^{T}_{f,j}$, and chemical exergy, $b_{ch,j}$ were calculated

under the conditions prevailing in the cardiac muscle ($pH = 7.27, T = 310.15K, and\ I = 0.14M$).

Cardiac muscle work performed (represented as $\oint W$ in Eq. (6)) is calculated from miniature Yucatan swine systemic and coronary hemodynamic responses of heart at rest and during graded treadmill exercise [35]. The mammalian heart functions as a double pump system to transport blood from the cardiac ventricles into the vascular system. This process involves the contraction (systole) and relaxation (diastole) phases, which generate a distinct pressure-volume curve for each cardiac cycle. The heart muscle has the capacity to convert both chemical and mechanical energy into work and heat. According to calculations treating the total power output of the cardiac system as a mechanical pump, the work performed during moderately intense exercise (5mph) is 3.20 times greater than at rest (Table 3). This information is consistent with the known physiology of the heart and its response to physical activity.

Exergy analysis of each component of a system helps to distinguish the endogenous irreversibilities from the exogenous [39]. Exergy destruction is considered to be endogenous irreversible exergy, which is an internal phenomenon caused by chemical reactions and heat transfer. Exergy losses of a system may be associated with the irreversibility of a system, exergy transfer from the overall system refers to the exportation of exergy that will be no longer used in the system to its surroundings. Exergy loss is calculated after subtracting the exergy that leaves the system, from exergy that enters the system [40] (In Eq. (7), $\sum (\dot{m}b)_{in} - \sum (\dot{m}b)_{out}$ the term is defined as exergy loss and $\dot{X_{dest}}$ is the endogenous exergy destruction within the system. In biological systems, exergy loss is referred to as the amount of chemical exergy that cannot be captured or invested via metabolism. The exergy loss rate did not show any substantial difference in response to the conditions. However, higher influx and outflux exergies during exercise indicated a higher metabolism rate (Fig. 4C and D-E) and correspondingly higher entropy generation. The exergy destruction rate was found to be higher during treadmill exercise, attributed to the higher rates of metabolism, power performed, and heat generation (Fig. 4A). Under both exercise and resting conditions, the exergy destruction rates were positively proportional, indicating a gradual minimization of exergy losses and destruction rates over time. This trend could be interpreted as an "adaptation" mechanism, where the generated heat is removed through blood flow to maintain homeostasis and prevent temperature increase.

The regulatory influence of the amounts of the ADP availability in the circulating medium has been assessed at rest and during exercise represented in Table 5. At rest the system consumes 0.69 W/kg exergy when we evaluate produced cardiac output and transfer exergy of metabolic heat, total exergy destroyed is equal to 0.66 W/kg and during exercise these thermodynamic indicators values increase to 1.32 W/kg and 1.24 W/kg, respectively. With considering the ratio of destroyed mitochondrial exergy to cell exergy showed (36% at rest and 49% during exercise), we were able to reach how much of total exergy destruction rate is coming from mitochondrial metabolism, 0.24 W/kg at rest and 0.61 W/kg during exercise. The mitochondrial energy metabolism involvement to systems total exergy destruction is ca. 2.54 times more during exercise compared to rest. Energy efficiency, $\eta_{energetic\_respiration}$, defined in this work conceptualizes to demonstrate how efficiently the system allocates respiration energy while doing work. The energy efficiency of respiration is calculated as the proportion of energy release of ATP hydrolysis to total energy release of aerobic respiration as described Eq. (12). During exercise the muscle system is 22% more efficient while converting aerobic respiration into work compared to rest ((Table 5) calculated as 58% during exercise and 36% at rest). Additionally, exergy efficiency of respiration $\eta_{exergetic\_respiration}$ was defined in the same manner this time taking account exergy release of ATP hydrolysis and total exergy release of aerobic respiration showing how efficiently available chemical exergy in the system is able to be used to produce energy. We showed that during exercise, the system is 18% more efficient while converting available exergy to useable exergy ((Table 5) calculated as 50% during exercise and 32% at rest). Increase in respiratory efficiencies, energetically and exergetically, during exercise is a consequence of higher levels of ADP in the circulating medium while power output is substantially increased compared to resting heart. The increase of the power output during exercise (ca. 3 times) leads to a substantial increase in the total rate of the exergy release of the muscle system due to the increase of respiratory activity and nearly double the rate of the exergy release via ATP hydrolysis. It was shown that increase of the total rate of the exergy release in the muscle due to respiratory activity, exergy destruction and entropy generation rate upon shifting to the exercised state from the resting state is not only driven by the regulatory influence of ADP amount and mainly affected by substantially increase of the power output. While the regulatory influence of the ADP ratio in the circulating medium has an appreciable effect on respiratory metabolism efficiencies. Both muscle models were investigated in terms of the ratio of metabolic thermal energy to net energy liberated. It revealed that the presence of more ADP concentration in the systems environment causes 24% of its net energy converted to metabolic heat while 29% of it is under lower ADP concentration. Based on observations of Hall and Guyton [41], stating this ratio of heat release from energy coming from food in a healthy human cell is maximum 0.35 under optimal conditions, but it was not known whether this ratio would be different when different conditions prevail. This above finding shows the resting system is very close to optimal conditions.

In the pioneering studies, muscle work efficiency was calculated either based on the first law of thermodynamics (Eq. (9)) as $\eta_I = \frac{W}{\Delta H}$, e.g., the ratio of work done by the heart to the chemical energy of nutrients consumed, or based on the second law efficiency (Eq. (10)) as $\eta_{II} = \frac{W}{W_{max}} = \frac{W}{\Delta} G$, e.g., the ratio of the work done by the system to the maximum work that the system can extract. Upon the experimental measurements in isolated muscle groups, the first law efficiency ranged between 0.14 and 0.35 and the second law efficiency ranged between 0.17 and 0.42 [18], where the theoretical maximum first and the second law efficiencies were 0.84 and 1.0 [13], respectively. To validate our conceptualized models are empirically realistic first and the second law efficiency analysis applied (Table 4). The first and second law efficiencies calculated in this study are consistent with the outcomes of the experimental research [18]. First law efficiency calculation demonstrated during exercise muscle is 6% more efficient (0.32 at rest and 0.38 during exercise). While Second law efficiency showed with higher level of energy precursor availability in a circulation medium makes exercise muscle 10% more efficient compared to resting. This simply points to muscle becoming more efficient with exercise when the necessary amount of energy precursor is available. Inefficiencies of muscle energy metabolism is mainly caused by inefficient ATP (or substrate) use [4,42]. The supporters of the idea also include failure in calcium transport, ADP diffusion and generation of localized ATP pools to

the causes of the impairment [4,42]. Additionally, cardiac muscle efficiency is defined in analogy with that of the engine efficiency and showed less than 25% variation [43].

Muscle machinery described in Fig. 1 is similar to a steam engine, where ADP + P_i is analogous to low-energy water and ATP is analogous to high-energy steam. ATP, ADP, and P_i are circulating between the site of the metabolic activity and the muscle machinery to interconnect them by serving like a circulating medium. The higher the amount and the circulation rate of the working medium, the higher would be the work performance rate. In the steam engine the amount and pressure of the steam at the inlet and the outlet of the turbine is usually constant, on the other hand in the muscle machinery, ATP, ADP and P_i concentrations are rarely constant. Moreover, a steam engine usually works under steady-state conditions and the muscle machinery described in this study runs under unsteady conditions most of the time. The impulse ATP input to mitochondria represents the real functioning mode of the muscle system in the body; therefore, the consequences of this study fills an important gap in our understanding of how energy extracted from the nutrients to muscle work.

There are conflicting reports in the literature regarding the relationship between ATP utilization and muscle work performance efficiency, most probably because of the variations in the experimental protocols. For example, Bangsbo et al. [44], suggested that the rate of ATP turnover increases during intense exercise at a constant work rate and the efficiency declines as intense exercise is continued. Furthermore, when intense exercise is repeated, there was a shift toward greater aerobic energy contribution, but the total ATP turnover was not significantly altered. Implying that different results were obtained even upon repeating the same experiment in two subsequent cases. Cells may hydrolyze the pre-synthesized metabolic ATP to fulfill intra- and extracellular tasks [16]. The presence or absence of the pre-synthesized ATP in the circulation medium may be the cause of the conflicting observations. Another source of conflict may be allocating the pre-synthesized ATP not only for muscle work performance but also for different cellular activities. The methodology employed in this study may eliminate the risk of starting a simulation before the same initial conditions are attained by the muscles in every experiment.

5. Concluding remarks

The analysis of metabolite pathways and thermodynamic systems is essential to understanding the efficiency of biological systems under different conditions. In particular, *in silico* models incorporating metabolic pathways and thermodynamics provide valuable insights into how varying levels of energy precursors affect the efficiency of glucose utilization. By analyzing the thermodynamic efficiency of a system, we can also gain insights into the system's ability to adapt to varying levels of energy or substrate availability and work conditions.

In this study, muscle-perturbed aerobic respiration systems were simulated under two conditions: rest and moderately intense exercise. The analysis of the maximum attainable work performance rate via Gibbs free energy change of complex IV reaction showed approximately a two-fold increase during exercise, reconfirming the efficient use of ADP at rest. Additionally, the maximum possible metabolic heat removal was calculated via the enthalpy change of the complex IV reaction, showing that more metabolic heat needs to be removed from the surface of the body during exercise.

The level of cellular phosphate metabolites is directly linked to the amount of ATP hydrolyzed and is linearly proportional to the muscle system's power output. The total intracellular and mitochondrial phosphate concentrations were examined over time in both rest and exercise states. Our analysis suggests high hexokinase activity in the cytoplasm and high H2PO-4/H+ cotransporter activity from the cytoplasm to the matrix, irrespective of the states.

Furthermore, the study showed that availability of higher amounts of ATP precursors ADP and intracellular inorganic phosphate in the cell pool enhances ATP production. During exercise, more oxygen is required to provide greater power since high-intensity metabolism prevails. Respiration energy calculated from rates of oxygen flux via complex IV reaction and its corresponding Gibbs free energy. We have demonstrated that muscle subjected to exercise allocates more energy for respiration, and this significant increase in energy allocation demonstrates an increase in the use of oxygen.

In conclusion, our simulations of muscle-perturbed aerobic respiration metabolism in different conditions suggest that metabolic pathways could be capable of adjusting energy metabolism rates via adjusting their rates of respiration and ATP utilization, for the efficient use of the energy or exergy extracted from the nutrients.

Author contribution statement

Bahar Hazal Yalcinkaya: Conceived and designed the experiments; Performed the experiments; Analyzed and interpreted the data; Contributed reagents, materials, analysis tools or data; Wrote the paper.

Seda Genc, Bayram Yılmaz, Mustafa Özilgen: Conceived and designed the experiments; Analyzed and interpreted the data; Contributed reagents, materials, analysis tools or data; Wrote the paper.

Funding statement

This study did not receive any specific funding or grant.

Data availability statement

Data will be made available on request.

Declaration of competing interest

The authors declare that they have no known competing financial interests or personal relationships that could have appeared to influence the work reported in this paper.

References

[1] S.L. Murphy, J. Xu, K.D. Kochanek, Deaths: final data for 2010, Nat. Vital Stat. Rep. Cent. Dis. Contr. Prev. Nat. Cent. Heal. Stat. Nat. Vital Stat. Sys. 61 (2013) 1e117.
[2] J. Xu, S.L. Murphy, B. Kenneth, D. Kochanek, B. Bastian, E. Arias, Deaths: final data for 2016, Nat. Vital Stat. Rep. Cent. Dis. Contr. Prev. Nat. Cent. Heal. Stat. Nat. Vital Stat. Sys. 67 (2018).
[3] M. Mariunas, K. Daunoravičienė, J. Griškevicius, J. Andrašiutė, Research of relation between muscle biosignal and systolic blood pressure, and application of its characteristics for evaluation of efficiency, J. Vibroeng 10 (2008).
[4] C.J. Barclay, Getting energy to where it is required is a problem in the failing heart, J. Physiol. 586 (2008) 5037–5503.
[5] J.P. Ribeiro, G.R. Chiappa, C.C. Callegaro, The contribution of inspiratory muscles function to exercise limitation in heart failure: pathophysiological mechanisms, Braz. J. Phys. Ther. 16 (2012) 261–267.
[6] G.A. Power, B.H. Dalton, C.L. Rice, Human neuromuscular structure and function in old age: a brief review, J. Sport Health Sci. 2 (2013) 215–226.
[7] G. Gouspillou, N. Sgarioto, S. Kapchinsky, F. Purves-Smith, B. Norris, C.H. Pion, et al., Increased sensitivity to mitochondrial permeability transition and myonuclear translocation of endonuclease G in atrophied muscle of physically active older humans, Faseb. J. 28 (2014) 1621–1633.
[8] G. Gouspillou, C. Scheede-Bergdahl, S. Spendiff, M. Vuda, B. Meehan, H. Mlynarski, et al., Anthracycline-containing chemotherapy causes long-term impairment of mitochondrial respiration and increased reactive oxygen species release in skeletal muscle, Sci. Rep. 5 (2015) 8717.
[9] R.T. Hepple, Mitochondrial involvement and impact in aging skeletal muscle, Front. Aging Neurosci. 6 (2014) 211.
[10] P.S. Brookes, Y. Yoon, J.L. Robotham, M.W. Anders, S.S. Sheu, Calcium, ATP, and ROS: a mitochondrial love-hate triangle, Am. J. Physiol. Cell Physiol. 287 (2004) C817–C833.
[11] B. Kadenbach, M. Huttemann, S. Arnold, I. Lee, E. Bender, Mitochondrial energy metabolism is regulated via nuclear-coded subunits of cytochrome c oxidase, free radical, Biol. Med. 29 (2000) 211–221.
[12] J. Çatak, M. Özilgen, A.B. Olcay, B. Yılmaz, Assessment of the work efficiency with exergy method in ageing muscles and healthy and enlarged hearts, Int. J. Exergy 25 (2018) 1–33.
[13] E. Sorgüven, M. Özilgen, First and second law work production efficiency of a muscle cell, Int. J. Exergy 18 (2015) 142–156.
[14] S. Genc, E. Sorguven, I.A. Kurnaz, M. Ozilgen, Exergetic efficiency of ATP production in neuronal glucose metabolism, Int. J. Exergy 13 (2013) 60–84.
[15] S. Genc, E. Sorguven, M. Ozilgen, I.A. Kurnaz, Unsteady exergy destruction of the neuron under dynamic stress conditions, Energy 59 (2013) 422–431.
[16] B.H. Yalçınkaya, S. Genc, J. Çatak, B. Yılmaz, M. Özilgen, Neural energy conversion in ibrahim dinçer, in: Comprehensive Energy Systems, first ed., Elsevier, 2018. ISBN: 9780128095973.
[17] A.J. Tarberner, J.-C. Han, D. Losielle, P.M.F. Nielsen, An innovative work-loop calorimeter for in vitro measurement of the mechanics and energetics of working cardiac trabeculae, J. Appl. Physiol. 111 (6) (2011) 1798–1803.
[18] N.P. Smith, C.J. Barclay, D.S. Loiselle, The efficiency of muscle contraction, Prog. Biophys. Mol. Biol. 1 (88) (2005) 1–58.
[19] B.H. Yalçınkaya, Erikli Ş, B.A. Özilgen, A.B. Olcay, E. Sorgüven, M. Özilgen, Thermodynamic analyses of the squid mantle muscles and giant axon during slow swimming and jet escape propulsion, Energy 102 (2016) 537–549.
[20] M. Schweiker, J. Kolarik, M. Dovjak, M. Shukuya, Unsteady-state human-body exergy consumption rate and its relation to subjective assessment of dynamic thermal environments, Energy Build. 116 (2016) 164–180.
[21] I.B. Henriques, C.E.K. Mady, S. de Oliveira Junior, Exergy model of the human heart, Energy 117 (2016) 612–619.
[22] A.S. Semerciöz, B. Yılmaz, M. Özilgen, Thermodynamic assessment of allocation of energy and exergy of the nutrients for the life processes during pregnancy, Br. J. Nutr. 124 (7) (2020) 742–753.
[23] C. Yildiz, M.E. Öngel, B. Yilmaz, M. Özilgen, Diet-dependent entropic assessment of athletes' lifespan, J. Nutr. Sci. 10 (2021).
[24] M. Prek, Thermodynamical analyses of human thermal comfort, Energy 31 (5) (2006) 732–743.
[25] C. Silva, K. Annamalai, Entropy generation and human aging: lifespan entropy and effect of physical activity level, Entropy 10 (2) (2008) 100–123.
[26] C.E.K. Mady, C. Albuquerque, T.L. Fernandes, A.J. Hernandez, P.H.N. Saldiva, J.I. Yanagihara, S. de Oliveira Jr., Exergy performance of human body under physical activities, Energy 62 (2013) 370–378.
[27] J. Çatak, A.Ç. Develi, E. Sorguven, M. Özilgen, H.S. İnal, Lifespan entropy generated by the masseter muscles during chewing: an indicator of the life expectancy? Int. J. Exergy 18 (1) (2015) 46–67.
[28] M.E. Öngel, C. Yıldız, C. Akpınaroğlu, B. Yilmaz, M. Özilgen, Why women may live longer than men do? A telomere-length regulated and diet-based entropic assessment, Clin. Nutr. 40 (3) (2021) 1186–1191.
[29] C. Yildiz, V.A. Bilgin, B. Yilmaz, M. Özilgen, Organisms live at far-from-equilibrium with their surroundings while maintaining homeostasis, importing exergy and exporting entropy, Int. J. Exergy 31 (3) (2020) 287–300.
[30] K.F. LaNoue, A.C. Schoolwerth, Metabolite transport in mitochondria, Annu. Rev. Biochem. 48 (1) (1979) 871–922.
[31] S. Bose, S. French, F.J. Evans, F. Joubert, R.S. Balaban, Metabolic network control of oxidative phosphorylation multiple roles of inorganic phosphate, J. Biol. Chem. 278 (2003) 39155–39165.
[32] D.A. Beard, Modeling of oxygen transport and cellular energetics explains observations on in vivo cardiac energy metabolism, PLoS Comput. Biol. 2 (9) (2006) e107.
[33] F. Wu, J.A. Jeneson, D.A. Beard, Oxidative ATP synthesis in skeletal muscle is controlled by substrate feedback, Am. J. Physiol. Cell Physiol. 292 (1) (2007) C115–C124.
[34] F. Wu, F. Yang, K.C. Vinnakota, D.A. Beard, Computer modeling of mitochondrial tricarboxylic acid cycle, oxidative phosphorylation, metabolite transport, and electrophysiology, J. Biol. Chem. 282 (2007) 24525–24537.
[35] S.B. Bender, M.J. van Houwelingen, D. Merkus, D.J. Duncker, M.H. Laughlin, Quantitative analysis of exercise-induced enhancement of early-and late-systolic retrograde coronary blood flow, J. Appl. Physiol. 108 (3) (2010) 507–514.
[36] R.A. Alberty, Thermodynamics of Biochemical Reactions, John Wiley & Sons, 2005.
[37] R.A. Alberty, Standard Gibbs free energy, enthalpy, and entropy changes as a function of pH and pMg for several reactions involving adenosine phosphates, J. Biol. Chem. 244 (1969) 3290–3302.
[38] J. Jeneson, H. Westerhoff, T. Brown, C. Van Echteld, R. Berger, Quasi-linear relationship between Gibbs free energy of ATP hydrolysis and power output in human forearm muscle, Am. J. Physiol. Cell Physiol. 268 (1995) C1474–C1484.
[39] T. Morosuk, G. Tsatsaronis, A new approach to the exergy analyses of absorption refrigeration machines, Energy 33 (2008) 890–907.
[40] L. Stougie, H.J. van der Kooi, Possibilities and consequences of the total cumulative exergy loss method in improving the sustainability of power generation, Energy Convers. Manag. 107 (2016) 60–66.
[41] J.E. Hall, A.C. Guyton, Guyton and Hall Textbook of Medical Physiology, thirteenth ed., Elsevier, USA, 2016.

[42] F. Joubert, J.R. Wilding, D. Fortin, V. Domergue-Dupont, M. Novotova, R. Ventura-Clapier, V. Veksler, Local energetic regulation of sarcoplasmic and myosin ATPase is differently impaired in rats with heart failure, J. Physiol. 586 (2008) 5181–5192.
[43] G. Ten Velden, G. Elzinga, N. Westerhof, Left ventricular energetics. Heat loss and temperature distribution of canine myocardium, Circ. Res. 50 (1982) 63–73.
[44] J. Bangsbo, P. Krustrup, J. González-Alonso, B. Saltin, ATP production and efficiency of human skeletal muscle during intense exercise: effect of previous exercise, Am. J. Physiol. Endocrinol. Metab. 280 (6) (2001) E956–E964.